



# Epimorphin Alters the Inhibitory Effects of SOX9 on Mmp13 in Activated Hepatic Stellate Cells

James Pritchett<sup>1,3,9</sup>, Varinder S. Athwal<sup>1,3,9</sup>, Emma Harvey<sup>1</sup>, Katherine Martin<sup>1,3</sup>, Jessica Llewellyn<sup>1,3</sup>, Philip Ireland<sup>1</sup>, Alexander Nicolaidis<sup>1</sup>, Martin J. Humphries<sup>4</sup>, Nicoletta Bobola<sup>2</sup>, Neil A. Hanley<sup>1,3</sup>, Karen Piper Hanley<sup>1,3\*</sup>

**1** Centre for Endocrinology and Diabetes, Manchester Academic Health Sciences Centre, University of Manchester, Manchester, United Kingdom, **2** School of Dentistry, Manchester Academic Health Sciences Centre, University of Manchester, Manchester, United Kingdom, **3** Manchester Biomedical Research Centre, Central Manchester University Hospitals NHS Foundation Trust, Manchester, United Kingdom, **4** Wellcome Trust Centre for Cell-Matrix Research, University of Manchester, Manchester, United Kingdom

## Abstract

**Background and Aims:** Liver fibrosis is a major cause of morbidity and mortality. It is characterised by excessive extracellular matrix (ECM) deposition from activated hepatic stellate cells (HSCs). Although potentially reversible, treatment remains limited. Understanding how ECM influences the pathogenesis of the disease may provide insight into novel therapeutic targets for the disease. The extracellular protein Epimorphin (EPIM) has been implicated in tissue repair mechanisms in several tissues, partially, through its ability to manipulate proteases. In this study, we have identified that EPIM modulates the ECM environment produced by activated hepatic stellate cells (HSCs), in part, through down-regulation of pro-fibrotic Sex-determining region Y-box 9 (SOX9).

**Methods:** Influence of EPIM on ECM was investigated in cultured primary rat HSCs. Activated HSCs were treated with recombinant EPIM or SOX9 siRNA. Core fibrotic factors were evaluated by immunoblotting, qPCR and chromatin immunoprecipitation (ChIP).

**Results:** During HSC activation EPIM became significantly decreased in contrast to pro-fibrotic markers SOX9, Collagen type 1 (COL1), and  $\alpha$ -Smooth muscle actin ( $\alpha$ -SMA). Treatment of activated HSCs with recombinant EPIM caused a reduction in  $\alpha$ -SMA, SOX9, COL1 and Osteopontin (OPN), while increasing expression of the collagenase matrix metalloproteinase 13 (MMP13). Sox9 abrogation in activated HSCs increased EPIM and MMP13 expression.

**Conclusion:** These data provide evidence for EPIM and SOX9 functioning by mutual negative feedback to regulate attributes of the quiescent or activated state of HSCs. Further understanding of EPIM's role may lead to opportunities to modulate SOX9 as a therapeutic avenue for liver fibrosis.

**Citation:** Pritchett J, Athwal VS, Harvey E, Martin K, Llewellyn J, et al. (2014) Epimorphin Alters the Inhibitory Effects of SOX9 on Mmp13 in Activated Hepatic Stellate Cells. PLoS ONE 9(6): e100091. doi:10.1371/journal.pone.0100091

**Editor:** Wing-Kin Syn, Institute of Hepatology, Foundation for Liver Research, United Kingdom

**Received:** September 24, 2013; **Accepted:** May 22, 2014; **Published:** June 27, 2014

**Copyright:** © 2014 Pritchett et al. This is an open-access article distributed under the terms of the Creative Commons Attribution License, which permits unrestricted use, distribution, and reproduction in any medium, provided the original author and source are credited.

**Funding:** This work was funded by the Medical Research Council (MRC; KPH, MR/J003352/1; VSA and KM are MRC Clinical Training Fellows); the Manchester Biomedical Research Centre; the Wellcome Trust (NAH, WT088566MA) and the Biological & Biotechnological Sciences Research Council (BBSRC; studentship to EH). The funders had no role in study design, data collection and analysis, decision to publish, or preparation of the manuscript.

**Competing Interests:** The authors have declared that no competing interests exist.

\* Email: karen.piperhanley@manchester.ac.uk

<sup>9</sup> These authors contributed equally to this work.

## Introduction

Fibrosis of the liver is a major cause of worldwide morbidity and mortality. End-stage disease can be treated by transplantation; however, there is a huge shortage of donor organs and focus on end-stage disease is too late. Urgent development of novel antifibrotic therapies is needed during reversible phases of the disease but none have been so far approved [1,2].

Liver fibrosis is a result of repetitive rounds of injury and attempted repair resulting in excessive extracellular matrix (ECM) deposition. One of the key cells mediating fibrosis is the hepatic stellate cell (HSC) [3,4]. Following injury to the liver, HSCs become activated into proliferative myofibroblasts (MFs), secrete

damaging ECM and infiltrate the surrounding tissue to cause fibrosis [3,4]. This process is regulated by multiple pathways and factors, including the transcription factor SOX9 (sex determining region Y-box 9) [5]. In response to pro-fibrotic cytokines, SOX9 becomes expressed in activated HSCs [6] where it regulates production of Collagen type 1 (COL1), the major collagen associated with the fibrotic scar [6], and Osteopontin (OPN) [7], a potential biomarker of liver disease and implicated in the progression of fibrosis [7–11]. In addition, factors capable of degrading matrix, matrix metalloproteinases (MMPs), and their inhibitors (tissue inhibitors of matrix metalloproteinases; TIMPs) are also altered to favor ECM accumulation [12]. Given its central importance, understanding how ECM components influence the

pathogenesis of fibrosis may provide insights into potential therapeutic strategies for liver fibrosis.

An ECM protein which has received attention as a modulator of tissue repair is Epimorphin (EPIM). Originally identified as a mesenchymal cell-surface associated protein [13], EPIM (also known as syntaxin 2) plays significant morphogenic roles in several tissues including skin, hair follicle, mammary gland, lung, kidney, intestine, pancreas and liver [14–16]. Although complex, evidence suggests EPIM has two distinct functions depending on its location. As an intracellular protein it is involved in vesicular transport. As an extracellular protein EPIM acts as a morphogen capable of signaling through the epidermal growth factor receptor (EGFR) and integrins [17].

In the adult liver, EPIM is expressed in the connective tissue surrounding blood vessels, along the sinusoidal lining where HSCs reside [18,19] and in mesenchyme surrounding the bile duct where it is thought to play a role in duct formation [15,20]. *In vivo*, there is a reduction in EPIM expression following liver injury and HSC activation [21]. However, in models of liver regeneration, EPIM also appears to increase later in HSCs highlighting a potential role during the recovery phase of tissue repair [21–23]. In line with this, a feature of EPIM in both renal and liver fibrosis is its ability to induce protease expression favoring collagen degradation and resolution of fibrosis [22,24,25]. Although this provides clues of EPIM's role in modulating the ECM in fibrosis the mechanisms by which it acts and is regulated are less clear.

In this study, we hypothesized that the role of EPIM to ameliorate fibrosis is mediated at least in part by an interplay with SOX9. We have investigated this *in vitro* in HSCs to demonstrate an inter-dependence governed by negative feedback that could be the focus of future work aimed a therapeutic intervention in liver fibrosis.

## Methods

### Primary cell culture

Primary rat hepatic stellate cells (rHSCs) were isolated and cultured as described previously [6,26] under project licence 40/3417 following approval by the University of Manchester local Ethical Review Committee. *Sox9* gene silencing was carried out using siRNA by Nucleofection (Amaxa Biosystems GmbH) as described previously [6]. For time course activation, cells were either immediately taken for protein analysis (time 0) or maintained in culture without passage for the desired time (3, 7 and 10 days) [6,7], whereas all other experiments (Chromatin immunoprecipitation, siRNA BrdU and EPIM) used culture-activated (7 days on tissue culture plastic, in 16% serum) rHSCs, passaged once. Following passage, rHSCs were treated for 24 hours with recombinant human EPIM (R&D Systems) or vehicle control (PBS) in 0% serum at 0.5 µg/ml, 1 µg/ml or 2 µg/ml or cultured on Matrigel substrate (6.6 mg/ml) for 2 weeks [27]. For BrdU incorporation, HSCs (activated and passaged as above) were plated onto fibronectin coated (5 µg/cm<sup>2</sup>; Sigma-Aldrich) glass chamber slides and left overnight in 16% serum [6]. HSCs were then cultured in serum free media in the presence or absence of 2 µg/ml rhEPIM (as above) with BrdU (30 µM) incorporation for the final 4 hours (in a total 24 hour EPIM treatment experiment). HSCs were washed and fixed in 4% PFA for immunohistochemistry as previously described [6]. BrdU positive cells were counted from 5 separate areas of each culture chamber at 10× magnification and numbers expressed as a percent of total cells counted per area.

### Animal Models of Liver Fibrosis

All *in vivo* experiments were carried out under UK Home Office Licence 40/3417 and approved by the University of Manchester local ethical review process. Male C57Bl/6J mice were given twice weekly intraperitoneal injections of carbon tetrachloride (CCl<sub>4</sub>) diluted 1:3 in olive oil, or vehicle control (2 µl/mg body weight) for 8 weeks. At the appropriate time point animals were killed by CO<sub>2</sub> asphyxiation and liver and serum samples were prepared for further analysis. Fibrosis was assessed from serum liver enzymes activities and histological Picrosirius Red (PSR) for total collagen and α-SMA staining for myofibroblasts, as previously described [28].

### Gene and Protein expression

For quantitative PCR (qPCR), RNA was isolated from cells using the RNeasy kit (Qiagen Ltd., West Sussex, UK). Following DNase I treatment, cDNA was synthesized from 1 µg of RNA with a RNA-to-cDNA kit (Applied Biosystems Ltd., Cheshire, UK). qPCR reactions were carried out on a StepOnePlus Real-Time PCR system (Applied Biosystems Ltd) using 1 µl of cDNA, intron-spanning primers wherever possible (Table S1), and SYBR green (PrimerDesign Ltd., Southampton, UK). Changes in mRNA expression were calculated using  $\Delta\Delta CT$  methodology relative to both *GusB* and  $\beta$ -actin [7,29].

Immunoblotting and quantification were performed as described previously [6,7], using denaturing SDS-PAGE, followed by transfer to nitrocellulose. Antibodies were diluted in PBS containing 0.1% tween and 5% milk powder. Membranes were probed with the appropriate HRP conjugated secondary antibody (GE Healthcare) and proteins visualised using chemiluminescence (ECL Prime, GE Healthcare). Quantification by densitometry was carried out using Qunattity One software (Biorad). Antibodies used are listed in Table S2.

### Chromatin immunoprecipitation

Chromatin immunoprecipitation (ChIP) assays were performed as described previously [7]. Briefly, sheared chromatin was isolated from rHSCs using an anti-SOX9 antibody (Santa Cruz Biotechnology Inc, CA). PCR was then performed using primers to amplify the conserved upstream element of *Mmp13* (Forward: TCCACAGCAAACACAAG Reverse: TTCATTCAAATATAAGAGTTCG). Fold enrichment of the conserved region in SOX9 ChIP samples versus negative control IgG ChIP was calculated relative to input chromatin, using  $\Delta\Delta Ct$  following qPCR as described elsewhere [30]. To quantify the effect of rhEPIM treatment on Sox9 binding to the conserved region of *Mmp13*, fold change in enrichment (% input) was calculated following qPCR in control versus rhEPIM treated ChIP samples.

### Statistical analysis

All experiments were carried out three times or more and, in the case of rHSCs, were investigated in different preparations of stellate cells from different animals. Data are expressed as means  $\pm$  SE and statistical significance was determined using two-tailed Student's *t* test where  $p < 0.05$  was considered significant.

## Results

### Epimorphin expression is decreased during activation of HSCs

We initially investigated the expression of EPIM in quiescent and 7 day activated rHSCs (Fig. 1A & B). In contrast to increased production of SOX9, α-Smooth muscle actin (α-SMA) and COLI

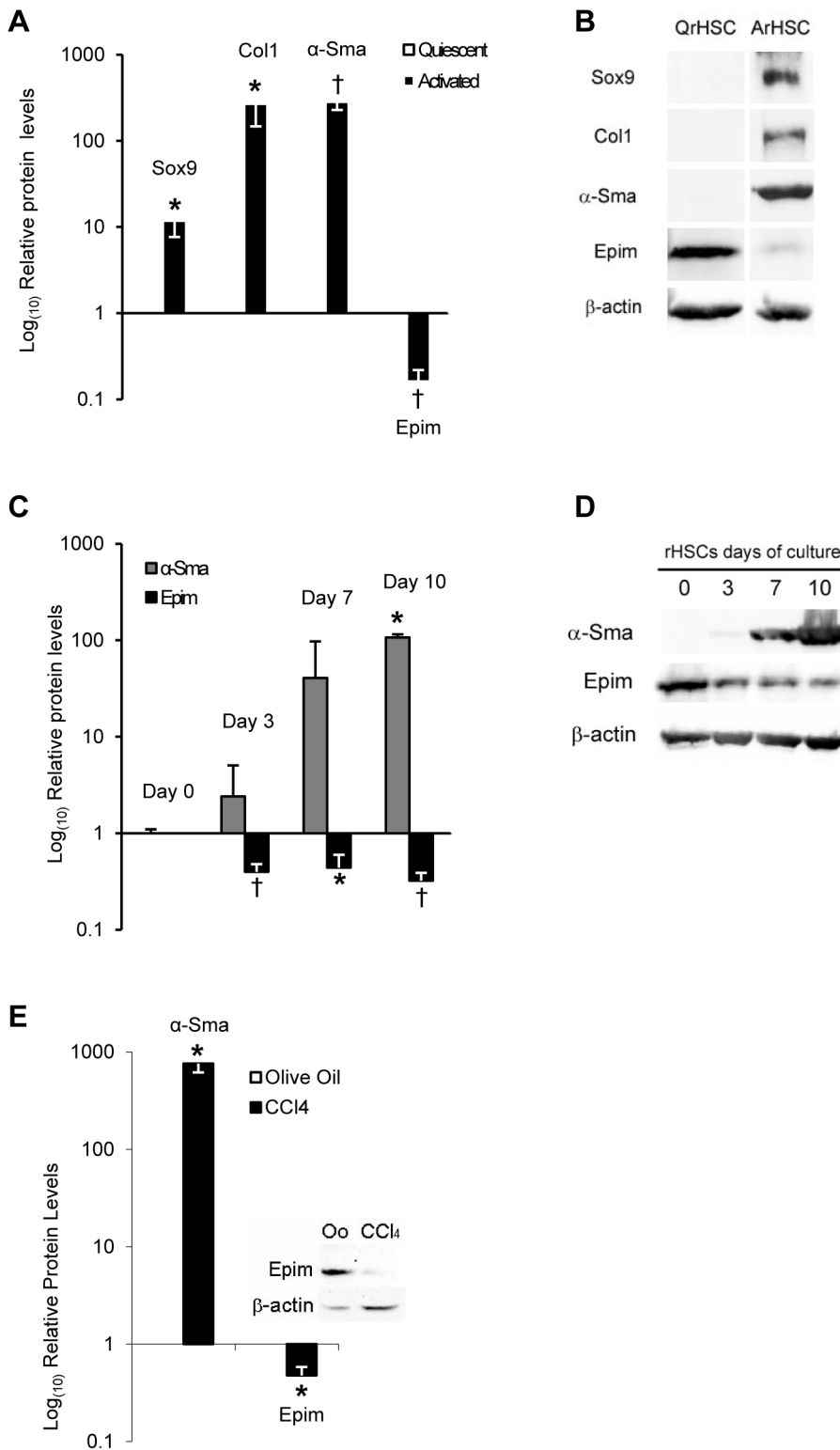


**Figure 1. EPIM expression in activated HSCs and fibrotic liver.** Quantification of proteins in rat HSCs and mouse whole liver lysates (rHSCs; A and C, mouse liver; E) and immunoblotting (rHSCs; B and D, mouse liver; E). (A) Induction of SOX9, COL1 and α-SMA with a reduction in EPIM in activated rat HSCs. Example immunoblot shown in (B). (C) Time course activation of rHSCs showing reduced EPIM levels in contrast to α-SMA (relative to day 0 quiescent; set at 1). Example immunoblot shown in (D). (E) Increased α-SMA protein in liver lysate from CCl<sub>4</sub> treated mice correlated with reduced EPIM protein levels (olive oil control is set at 1). Example EPIM immunoblot shown (inset E). α-SMA immunoblot shown in Figure 1B. All quantification was normalized to β-actin. \*, p<0.05, †, p<0.005. doi:10.1371/journal.pone.0100091.g001

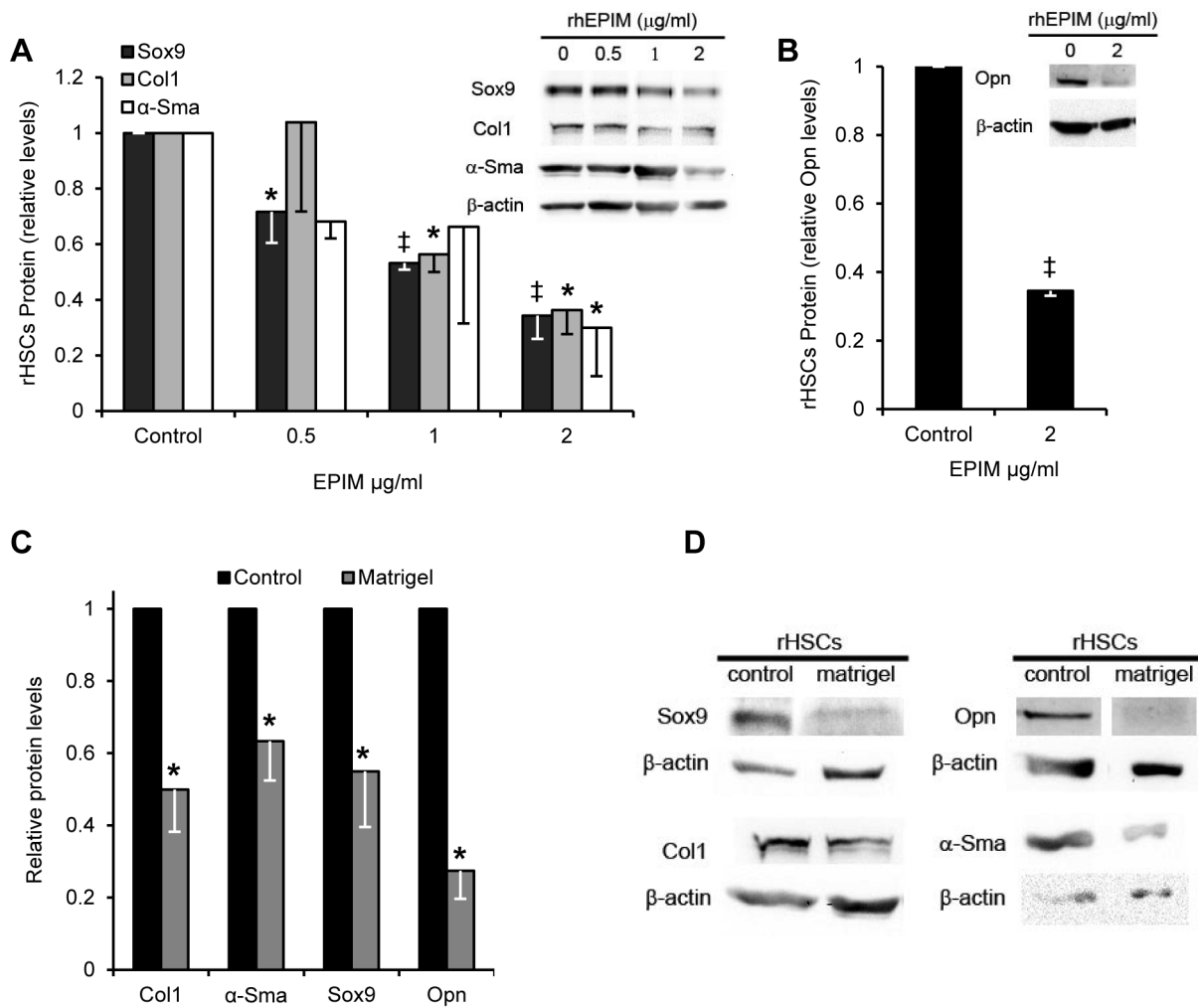


**Figure 2. EPIM alters the pro-fibrotic profile of activated HSCs.** (A and B) Quantification of pro-fibrotic proteins showing decreased SOX9, COL1 and  $\alpha$ -SMA in activated rHSCs following rhEPIM treatment. (B) Highest rhEPIM dose reduced OPN protein by ~65%. Example immunoblot for quantification shown (inset in A and B). (C and D) Quantification (C) and immunoblot (D) indicating decreased expression of COL1,  $\alpha$ -SMA, SOX9 and OPN following rHSCs culture on Matrigel for 14 days. All immunoblotting quantification was normalized to  $\beta$ -actin. \*,  $p < 0.05$ , ‡,  $p < 0.001$ . doi:10.1371/journal.pone.0100091.g002

proteins, we detected an 84% decrease in full length 34 KDa EPIM in activated rHSCs (Fig. 1A & B). The EPIM levels of quiescent rHSCs were reduced by 3 days of activation, before cells were fully activated as shown by intermediate levels of  $\alpha$ -SMA (Fig. 1C & D) SOX9, COL1 and OPN [6,7]. Moreover, compared to control, EPIM was almost absent in protein lysates from mice with fibrosis induced by CCl<sub>4</sub> injection (Fig. 1E; Figure S1).

#### Epimorphin decreases expression of pro-fibrotic genes in HSCs

EPIM's association with the quiescent HSC phenotype [18,21] and its role as a secreted extracellular factor led us to determine whether recombinant human EPIM (rhEPIM) added to the culture media was capable of inducing a quiescent-like phenotype in activated rHSCs. Treatment of 7 day activated rHSCs with rhEPIM resulted in a dose-dependent decrease in SOX9, COL1 and  $\alpha$ -SMA proteins (Fig. 2A). 2  $\mu$ g/ml rhEPIM reduced this pro-fibrotic protein profile by >60% from control levels (Fig. 2A). rhEPIM (2  $\mu$ g/ml) also reduced a OPN levels by 65% (Fig. 2B). These data are remarkably similar to culturing activated HSCs on Matrigel [31–34], known to contain EPIM [35], rather than tissue

culture plastic (Fig. 2C–D). These data concur with previous studies that have indicated activated HSCs cultured on soft substrates such as Matrigel can be 'deactivated' to a more quiescent-like state with greatly reduced  $\alpha$ -SMA and COL1 expression [31–34].

#### Epimorphin increases expression of proteases that cause collagen breakdown

To characterize rhEPIM-treated HSCs further we investigated the expression of genes previously associated with an inactive or deactivated HSC phenotype as indicative of the recovery phase following liver injury [36,37]. We detected few changes in gene expression characteristic of this phenomenon (i.e. increased *Ggap*, *Ppar $\gamma$*  or *Bambi*; or decreased *Svep1* or *Cyp11B1*). EPIM did increase expression of pro-survival gene *Hspa1a/b* (Fig. 3A). However, there was no difference in total HSP70 protein, encompassing HSPA1a/b, or any difference in apoptosis as determined by the ratio of full length to cleaved Caspase 3 or proliferation determined by BrdU incorporation (Fig. S2A–C). In addition, activated HSCs treated with EPIM decreased *Ppar $\gamma$*  mRNA suggestive of a more myofibroblastic phenotype. However, we did not see any change

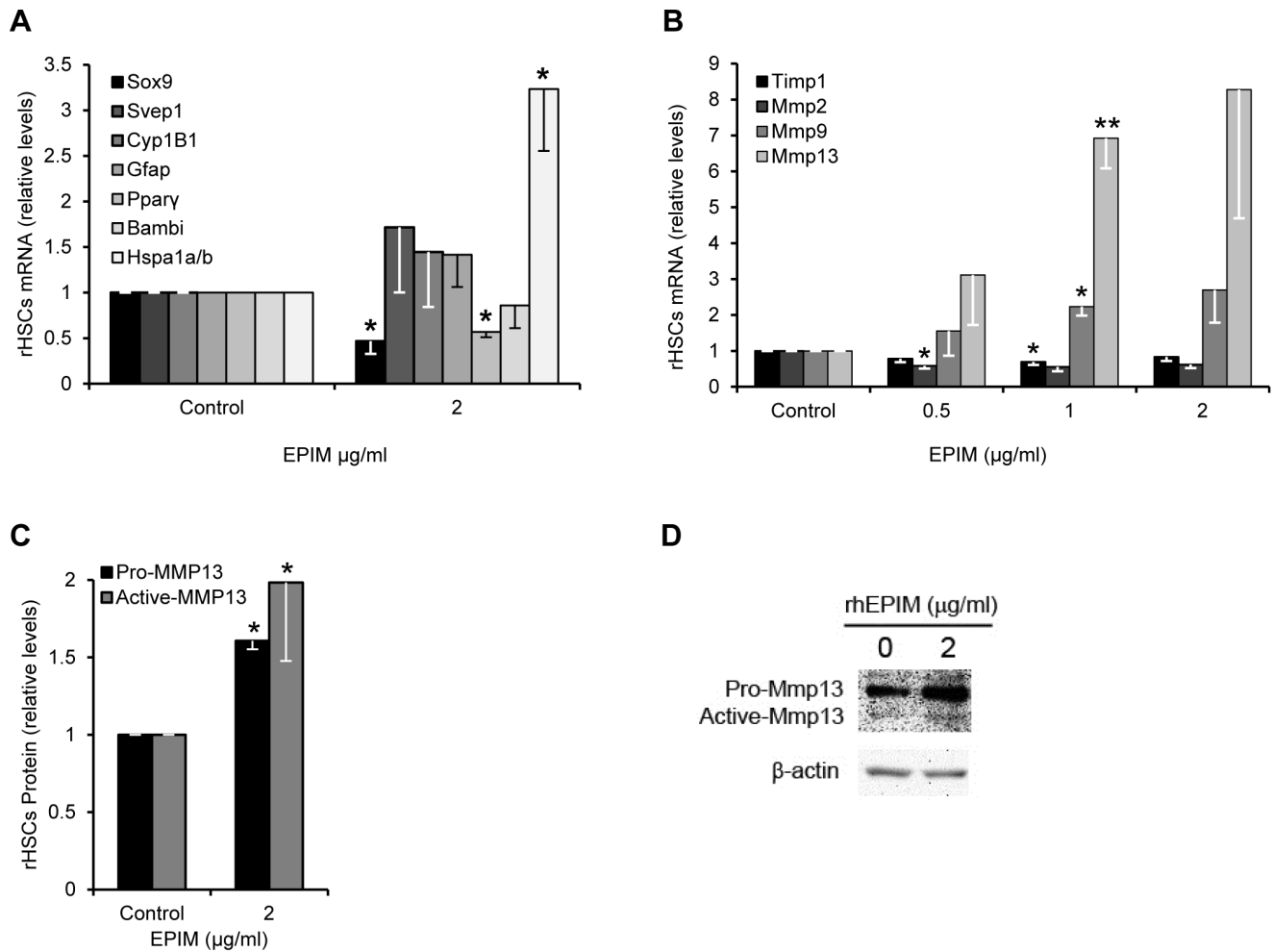


**Figure 3. EPIM increases *Mmp13* expression in activated HSC.** (A and B) Quantification of gene expression by qPCR in rhEPIM-treated activated rHSCs. *Hspa1a/b* expression was significantly increased (A), as were the proteases *Mmp9* and *Mmp13* (B) in response to rhEPIM. (C) Quantification of pro and active forms of MMP13 protein in rhEPIM-treated activated rHSCs. Both pro and active MMP13 protein levels were significantly increased. Example immunoblot shown in (D). \*,  $p < 0.05$  and \*\*,  $p < 0.01$ . doi:10.1371/journal.pone.0100091.g003

in *Pparγ* gene expression at other concentrations of EPIM treatment (Fig. S2D) and the levels of *Pparγ* transcripts in activated HSCs were already very low. In line with this there was no change in gross cell morphology or lipid accumulation by oil red O staining in EPIM treated HSCs (data not shown).

Studies have suggested Epim facilitates the recovery phase following liver injury [22]. It has been associated with resolution of fibrosis in both kidney and liver by inducing protease expression to cause ECM degradation [22,24]. In line with this, we detected altered MMP/TIMP expression in activated rHSCs treated with rhEPIM (Fig. 3B). Whereas expression of *Timp1* and *Mmp2* mRNA appeared to decrease following rhEPIM treatment, levels of *Mmp9* and *Mmp13* mRNA were increased (Fig. 3B). 1  $\mu\text{g/ml}$  of rhEPIM significantly induced *Mmp9* and *Mmp13* by 2.7 and 7.2 fold respectively. Similarly, MMP13 protein was increased following rhEPIM treatment (pro-MMP13 by 1.6 fold and active-MMP13 by 2 fold; Fig. 3C & D). In rodents MMP13 is the primary interstitial collagenase and thought to be a key enzyme involved in ECM resolution [4]. During liver fibrosis, MMP13 is thought to be transiently increased during initial stages but becomes almost undetectable with progressive disease, coincident with an increase in TIMPs 1 & 2 [38–40]. In activated HSCs, both pro and active

MMP13 were decreased (40% and 30% respectively; Fig. S3A). Conversely, similar to EPIM-treated activated HSCs, culturing cells on Matrigel increased pro and, to a lower extent, active forms of MMP13 (Fig. S3B).

### SOX9 limits levels of Epim and *Mmp13* in activated HSCs

Given the reduction in EPIM as SOX9 becomes expressed in activated HSCs (Fig. 1A–B); we investigated whether EPIM was a downstream target of SOX9. *Sox9* silencing resulted in a 1.6 fold induction of EPIM protein (Fig. 4A & D). In silico analysis did not identify a SOX9 element within 10 kb of the human *EPIM* gene. However, although SOX9 siRNA treated activated HSCs demonstrated little change in the profibrotic enzymes *Mmp2*, *Mmp9* and *Timp1*, there was a significant >2 fold increase in *Mmp13* mRNA (Fig. 4B). Similarly, pro and active MMP13 protein was increased >1.2 and 1.5 fold respectively in response to *Sox9* abrogation (Fig. 4C and D). A conserved SOX9 binding motif was identified in intron 7 of *MMP13* (Fig. 5A) which bound SOX9 with a 3-fold enrichment following SOX9 ChIP (Fig. 5B). In contrast, treatment of HSCs with rhEPIM reduced the association of endogenous SOX9 with the *MMP13* gene by 56%.

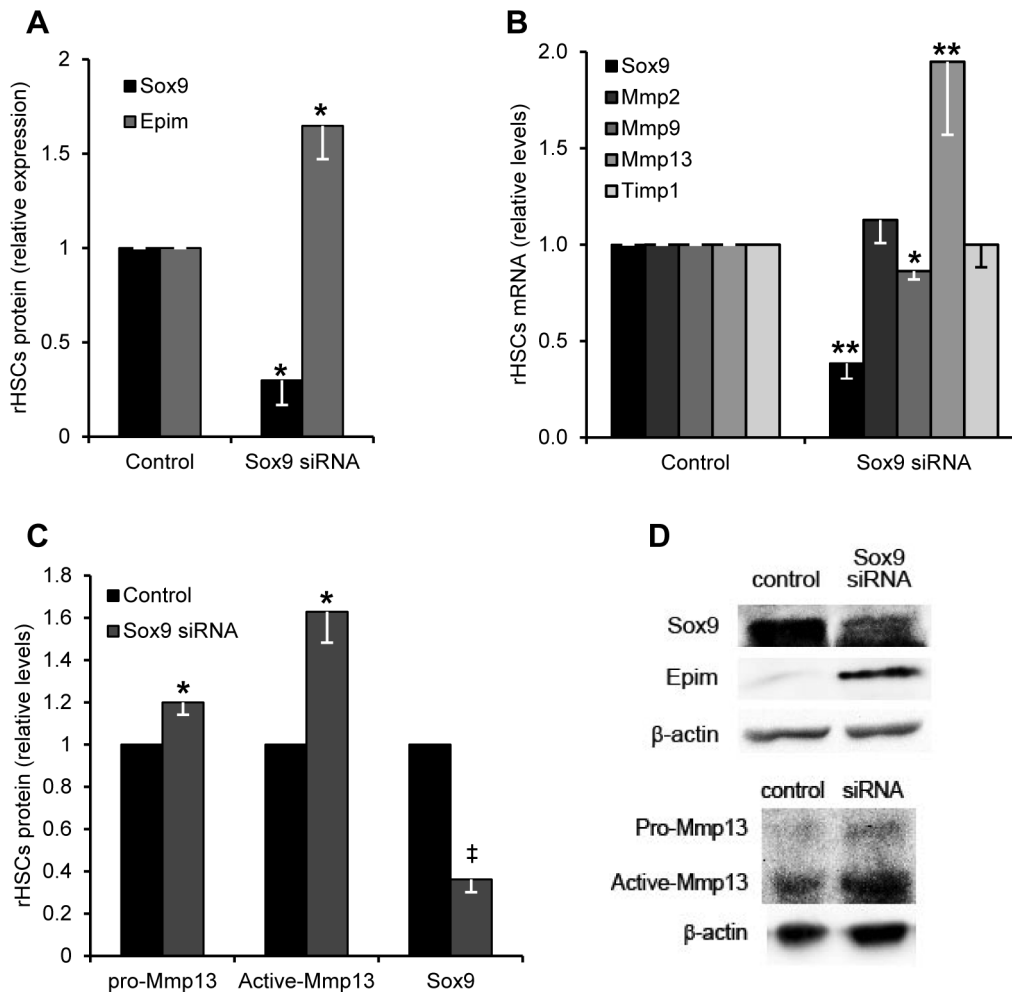


**Figure 4. SOX9 knockdown increases EPIM and MMP13 expression in activated HSCs.** Quantification of proteins (A and C) and genes (B) following siRNA abrogation of SOX9 in activated rHSCs standardized against scrambled siRNA control. Abrogation of SOX9 increases EPIM protein (A) and *Mmp13* mRNA and protein (B and C). (D) Example immunoblot shown for (A) and (C). Immunoblotting quantification was normalized to  $\beta$ -actin. \*,  $p < 0.05$  and \*\*,  $p < 0.01$ .

doi:10.1371/journal.pone.0100091.g004

## Discussion

Liver fibrosis is a common step in the progression of the majority of chronic liver diseases. Despite this, there are no approved therapies to reduce or remove the characteristic scar associated with tissue damage. EPIM has been implicated in tissue repair mechanisms following injury to lung, kidney or liver [18,22,24,41]. Previously, we have described how the transcription factor SOX9 regulates profibrotic proteins COL1 and OPN, in activated HSCs [6,7]. In this study, we show that EPIM ameliorates the profibrotic phenotype of HSCs and, specifically, decreases SOX9 levels. Conversely, we demonstrate that the presence of SOX9 in activated HSCs limits the amount of EPIM production. Taken together these data support a model of interdependent states of high and low EPIM and SOX9 in determining whether ECM is deposited or degraded in liver fibrosis (Figure 6).

Our investigations were prompted by reports that EPIM was increased in the recovery phase following liver injury [22] when some HSCs are proposed to escape apoptosis and revert to a quiescent-like state [36,37]. However, although our analysis of genes reported as characteristic of inactive or reverted HSCs [36,37] only detected an increase in the pro-survival gene *Hspa1a/l*

*b*, we detected no change in HSP70 protein expression in rhEPIM-treated HSCs or any difference in apoptosis by Caspase 3 expression or proliferation by BrdU incorporation. Of interest, we also detected a decrease in the adipogenic gene *Ppar $\gamma$* , associated with vitamin A uptake and lipid droplet formation in quiescent HSCs. Although, transcript levels of *Ppar $\gamma$*  in activated HSCs were already low potentially reflecting the detection limit for this study, the reduced availability of growth factors using serum free conditions may have also influenced *Ppar $\gamma$*  expression levels. However, in support of this we did not observe any change in gross cell morphology or lipid accumulation by oil red O staining. Moreover, our data showed that the more quiescent-like phenotype induced by EPIM in vitro is defined by reduced expression of the profibrotic genes *Sox9*,  *$\alpha$ -Sma*, *Col1* and *Opn*; similar to our observations from culturing activated HSCs on Matrigel. EPIM also increased *Mmp13* expression. Thus, our data imply EPIM's major role in cells adopting a quiescent phenotype is in altering the balance between the production of collagen and a protease that digests it [21,22,24]. In line with this, we also detected more modest alterations in proteases favoring a less fibrotic phenotype with reduced *Timp1* and *Mmp2* and increased *Mmp9* expression in response to EPIM.

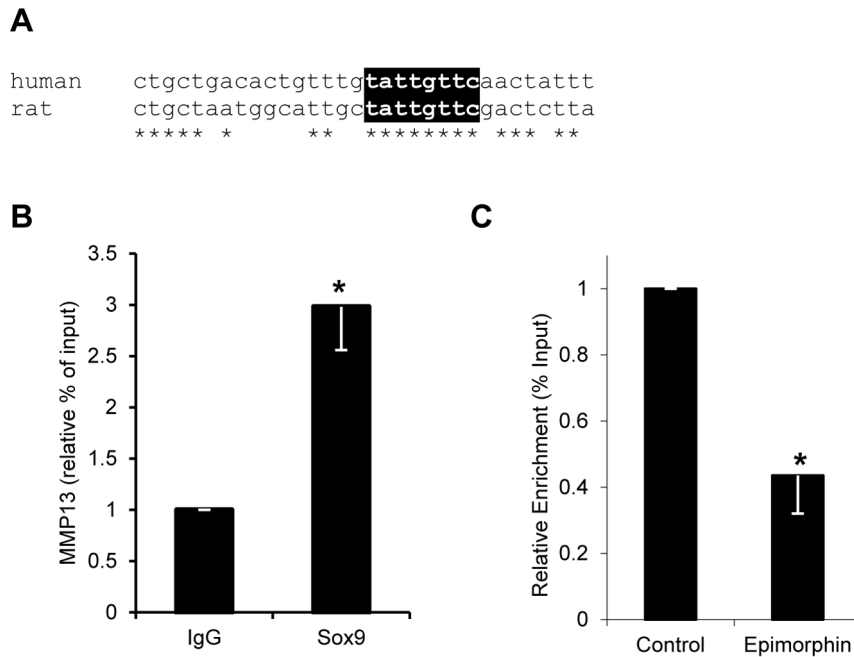


**Figure 5. Sox9 directly binds to *Mmp13* in activated HSCs.** (A) Alignment of a region within intron 7 of the *MMP13* gene with conserved SOX9-binding motif highlighted in black. Conserved nucleotides are indicated by asterisks (\*). (B and C) ChIP-qPCR for SOX9-binding element in conserved region of *MMP13* in activated rHSCs. (B) Fold enrichment of *MMP13* over IgG negative control antibody (IgG) is shown for SOX9-bound region (SOX9). (C) Relative change in enrichment (% Input) of the SOX9-binding element in control versus rhEPIM treated activated rHSCs. \*,  $p < 0.05$ . doi:10.1371/journal.pone.0100091.g005

Similar to rhEPIM treated HSCs, elevated EPIM following SOX9 abrogation also increased *Mmp13* expression. Given that SOX9 was capable of directly binding to a conserved motif in the *MMP13* gene; potentially SOX9's effect on lowering MMP13 expression in activated HSCs could be either direct, indirect via Epim or both. Our data are concordant with chondrogenesis during development when SOX9 plays a key role in regulating cell proliferation and the expression of cartilage matrix genes [5]; in

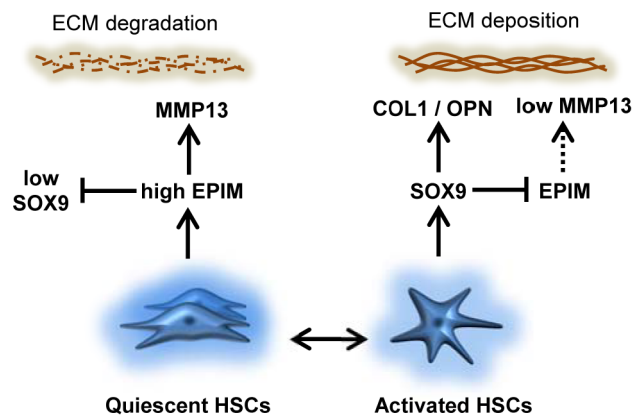


**Figure 6. Schematic representation of the opposing roles of SOX9 and EPIM during liver fibrosis.** The extracellular environment in the uninjured liver contains high levels of EPIM in quiescent HSCs and maintains a balance favoring ECM degradation through SOX9 inhibition and MMP13 expression. In contrast, as HSCs become activated following injury to the liver, EPIM is greatly reduced by the presence of SOX9 which favors ECM deposition rather than degradation. In addition to what is depicted via EPIM, high and low levels of SOX9 may directly repress and de-repress MMP13 expression respectively. doi:10.1371/journal.pone.0100091.g006

the later stages of chondrocyte maturation SOX9 is absent concomitant with an increase in MMP13 [42,43]. In contrast to our data, retroviral transfer of SOX9 in chick fibroblasts increased EPIM expression in cells cultured as pellets [21]. However, no change in EPIM was detected in response to SOX9 transduction of cells cultured in monolayer. In our studies, we would hypothesize that culturing activated HSCs on Matrigel would induce re-expression of EPIM. Unfortunately we could not test this because Matrigel contained confounding amounts of EPIM.

Taken together, our data support a broad role for SOX9 in ECM deposition (e.g. increased COL1 and OPN) and inhibiting degradation, Epim-induced mediated by proteases. Given there are currently no approved effective antifibrotic drugs to treat liver fibrosis [2,44], this study raises clinical possibilities. For instance, as a potential antifibrotic target, studies suggest enhanced expression of MMP13 attenuates liver fibrosis with reduced collagen levels [45,46]. Attenuation of SOX9 might represent a more attractive target capable of both reducing scar formation by decreasing ECM deposition and increasing its degradation.

## Supporting Information

**Figure S1 Liver Fibrosis in CCl<sub>4</sub> treated mice.** (A) Picro Sirius Red staining shows increased collagen deposition in liver sections from CCl<sub>4</sub> treated mice (dark grey areas of scar), versus vehicle control (Oo – Olive Oil). (B) Immunoblot showing increased  $\alpha$ -SMA protein in whole liver lysate from mice treated with CCl<sub>4</sub> versus vehicle control (Oo). Loading control is  $\beta$ -actin. (TIF)

**Figure S2 HSPA1a/b levels, apoptosis and proliferation are unchanged following rhEPIM treatment.** (A and B) Immunoblots showing two independent experiments of activated rHSCs treated with 2  $\mu$ g/ml of rhEPIM. (A) HSPA1a/b was unchanged.  $\beta$ -actin control is shown for protein loading. (B) no

alteration in full length or cleaved Caspase 3 was detected in response to rhEPIM. (C) activated rHSC proliferation was unchanged following EPIM treatment (2  $\mu\text{g}/\text{ml}$ ) indicated by cell numbers incorporating BrdU. Expressed as a percent of total cell numbers ( $n = 4$ ). (D) Quantification of gene expression by qPCR in 0.5  $\mu\text{g}/\text{ml}$  and 1  $\mu\text{g}/\text{ml}$  rhEPIM-treated activated rHSCs (\*,  $p < 0.05$ ). (TIF)

**Figure S3 MMP13 expression is reduced in activated HSCs.** (A and B) Quantification of MMP13 in rHSCs. (A) Reduction in pro and active forms of MMP13 following activation of rHSCs. (B) Increased expression of both pro and active-MMP13 in activated rHSCs cultured on Matrigel for 14 days. Example

## References

- Cohen-Naftaly M, Friedman SL (2011) Current status of novel antifibrotic therapies in patients with chronic liver disease. *Therap Adv Gastroenterol* 4: 391–417.
- Friedman SL, Sheppard D, Duffield JS, Violette S (2013) Therapy for fibrotic diseases: nearing the starting line. *Sci Transl Med* 5: 167sr161.
- Friedman SL (2008) Mechanisms of hepatic fibrogenesis. *Gastroenterology* 134: 1655–1669.
- Iredale JP (2007) Models of liver fibrosis: exploring the dynamic nature of inflammation and repair in a solid organ. *J Clin Invest* 117: 539–548.
- Pritchett J, Athwal V, Roberts N, Hanley NA, Hanley KP (2011) Understanding the role of SOX9 in acquired diseases: lessons from development. *Trends Mol Med* 17: 166–174.
- Piper Hanley K, Oakley F, Sugden S, Wilson DI, Mann DA, et al. (2008) Ectopic SOX9 Mediates Extracellular Matrix Deposition Characteristic of Organ Fibrosis. *Journal of Biological Chemistry* 283: 14063–14071.
- Pritchett J, Harvey E, Athwal V, Berry A, Rowe C, et al. (2012) Osteopontin is a novel downstream target of SOX9 with diagnostic implications for progression of liver fibrosis in humans. *Hepatology* 56: 1108–1116.
- Huang W, Zhu G, Huang M, Lou G, Liu Y, et al. (2010) Plasma osteopontin concentration correlates with the severity of hepatic fibrosis and inflammation in HCV-infected subjects. *Clin Chim Acta* 411: 675–678.
- Xie H, Song J, Du R, Liu K, Wang J, et al. (2007) Prognostic significance of osteopontin in hepatitis B virus-related hepatocellular carcinoma. *Dig Liver Dis* 39: 167–172.
- Zhao L, Li T, Wang Y, Pan Y, Ning H, et al. (2008) Elevated plasma osteopontin level is predictive of cirrhosis in patients with hepatitis B infection. *Int J Clin Pract* 62: 1056–1062.
- Syn WK, Choi SS, Liaskou E, Karaca GF, Agboola KM, et al. (2011) Osteopontin is induced by hedgehog pathway activation and promotes fibrosis progression in nonalcoholic steatohepatitis. *Hepatology* 53: 106–115.
- Iredale JP (2001) Hepatic stellate cell behavior during resolution of liver injury. *Semin Liver Dis* 21: 427–436.
- Hirai Y, Takebe K, Takashima M, Kobayashi S, Takeichi M (1992) Epimorphin: a mesenchymal protein essential for epithelial morphogenesis. *Cell* 69: 471–481.
- Radisky DC, Hirai Y, Bissell MJ (2003) Delivering the message: epimorphin and mammary epithelial morphogenesis. *Trends Cell Biol* 13: 426–434.
- Jia Y, Yao H, Zhou J, Chen L, Zeng Q, et al. (2011) Role of epimorphin in bile duct formation of rat liver epithelial stem-like cells: involvement of small G protein RhoA and C/EBPbeta. *J Cell Physiol*.
- Zhou J, Zhao L, Qin L, Wang J, Jia Y, et al. (2011) Epimorphin regulates bile duct formation via effects on mitosis orientation in rat liver epithelial stem-like cells. *PLoS One* 5: e9732.
- Radisky DC, Stallings-Mann M, Hirai Y, Bissell MJ (2009) Single proteins might have dual but related functions in intracellular and extracellular microenvironments. *Nat Rev Mol Cell Biol* 10: 228–234.
- Segawa D, Miura K, Goto T, Ohshima S, Mikami K, et al. (2005) Distribution and isoforms of epimorphin in carbon tetrachloride-induced acute liver injury in mice. *J Gastroenterol Hepatol* 20: 1769–1780.
- Hirose M, Watanabe S, Oide H, Kitamura T, Miyazaki A, et al. (1996) A new function of Ito cells in liver morphogenesis: evidence using a novel morphogenic protein, epimorphin, in vitro. *Biochem Biophys Res Commun* 225: 155–160.
- Zhou J, Zhao L, Qin L, Wang J, Jia Y, et al. (2010) Epimorphin regulates bile duct formation via effects on mitosis orientation in rat liver epithelial stem-like cells. *PLoS One* 5: e9732.
- Yoshino R, Miura K, Segawa D, Hirai Y, Goto T, et al. (2006) Epimorphin expression and stellate cell status in mouse liver injury. *Hepatol Res* 34: 238–249.
- Miura K, Yoshino R, Hirai Y, Goto T, Ohshima S, et al. (2007) Epimorphin, a morphogenic protein, induces proteases in rodent hepatocytes through NF-kappaB. *J Hepatol* 47: 834–843.

immunoblots are shown in inset (A and B). \*,  $p < 0.05$ , \*\*\*,  $p < 0.005$ . (TIF)

**Table S1 qPCR primers.**  
(DOC)

**Table S2 Antibodies and dilutions for immunoblotting.**  
(DOC)

## Author Contributions

Conceived and designed the experiments: KPH JP VSA. Performed the experiments: JP VSA EH KM PI AN JL. Analyzed the data: KPH JP VSA EH NB. Contributed reagents/materials/analysis tools: KPH MJH NAH NB. Wrote the paper: KPH MJH NAH NB.

- Watanabe S, Hirose M, Wang XE, Ikejima K, Oide H, et al. (1998) A novel hepatic stellate (Ito) cell-derived protein, epimorphin, plays a key role in the late stages of liver regeneration. *Biochem Biophys Res Commun* 250: 486–490.
- Yamada M, Oda T, Higashi K, Kushiya T, Yamakami K, et al. (2010) Involvement of epimorphin in the repair of experimental renal fibrosis in mice. *Lab Invest* 90: 867–880.
- Jia YL, Shi L, Zhou JN, Fu CJ, Chen L, et al. (2011) Epimorphin promotes human hepatocellular carcinoma invasion and metastasis through activation of focal adhesion kinase/extracellular signal-regulated kinase/matrix metalloproteinase-9 axis. *Hepatology* 54: 1808–1818.
- Smart DE, Green K, Oakley F, Weitzman JB, Yaniv M, et al. (2006) JunD is a profibrogenic transcription factor regulated by Jun N-terminal kinase-independent phosphorylation. *Hepatology* 44: 1432–1440.
- Rowe C, Gerrard DT, Jenkins R, Berry A, Durkin K, et al. (2013) Proteome-wide analyses of human hepatocytes during differentiation and dedifferentiation. *Hepatology* 58: 799–809.
- Oakley F, Meso M, Iredale JP, Green K, Marek CJ, et al. (2005) Inhibition of inhibitor of kappaB kinases stimulates hepatic stellate cell apoptosis and accelerated recovery from rat liver fibrosis. *Gastroenterology* 128: 108–120.
- Piper Hanley K, Hearn T, Berry A, Carvell MJ, Patch AM, et al. (2010) In vitro expression of NGN3 identifies RAB3B as the predominant Ras-associated GTP-binding protein 3 family member in human islets. *J Endocrinol* 207: 151–161.
- Donaldson IJ, Amin S, Hensman JJ, Kutejova E, Rattray M, et al. (2012) Genome-wide occupancy links Hoxa2 to Wnt-beta-catenin signaling in mouse embryonic development. *Nucleic Acids Res* 40: 3990–4001.
- Friedman SL, Roll FJ, Boyles J, Arenson DM, Bissell DM (1989) Maintenance of differentiated phenotype of cultured rat hepatic lipocytes by basement membrane matrix. *J Biol Chem* 264: 10756–10762.
- Gaca MD, Zhou X, Issa R, Kiriella K, Iredale JP, et al. (2003) Basement membrane-like matrix inhibits proliferation and collagen synthesis by activated rat hepatic stellate cells: evidence for matrix-dependent deactivation of stellate cells. *Matrix Biol* 22: 229–239.
- Shimada H, Rajagopalan LE (2012) Employment of gene expression profiling to identify transcriptional regulators of hepatic stellate cells. *Fibrogenesis Tissue Repair* 5 Suppl 1: S12.
- Sohara N, Znoyko I, Levy MT, Trojanowska M, Reuben A (2002) Reversal of activation of human myofibroblast-like cells by culture on a basement membrane-like substrate. *J Hepatol* 37: 214–221.
- Hirai Y (1993) Molecular cloning of human epimorphin: identification of isoforms and their unique properties. *Biochem Biophys Res Commun* 191: 1332–1337.
- Kisseleva T, Cong M, Paik Y, Scholten D, Jiang C, et al. (2012) Myofibroblasts revert to an inactive phenotype during regression of liver fibrosis. *Proc Natl Acad Sci U S A* 109: 9448–9453.
- Troeger JS, Mederacke I, Gwak GY, Dapito DH, Mu X, et al. (2012) Deactivation of hepatic stellate cells during liver fibrosis resolution in mice. *Gastroenterology* 143: 1073–1083 e1022.
- Iredale JP, Murphy G, Hembry RM, Friedman SL, Arthur MJ (1992) Human hepatic lipocytes synthesize tissue inhibitor of metalloproteinases-1. Implications for regulation of matrix degradation in liver. *J Clin Invest* 90: 282–287.
- Kossakowska AE, Edwards DR, Lee SS, Urbanski LS, Stabler AL, et al. (1998) Altered balance between matrix metalloproteinases and their inhibitors in experimental biliary fibrosis. *Am J Pathol* 153: 1895–1902.
- Watanabe T, Niioka M, Hozawa S, Kameyama K, Hayashi T, et al. (2000) Gene expression of interstitial collagenase in both progressive and recovery phase of rat liver fibrosis induced by carbon tetrachloride. *J Hepatol* 33: 224–235.
- Terasaki Y, Fukuda Y, Ishizaki M, Yamanaka N (2000) Increased expression of epimorphin in bleomycin-induced pulmonary fibrosis in mice. *Am J Respir Cell Mol Biol* 23: 168–174.



42. Hattori T, Muller C, Gebhard S, Bauer E, Pausch F, et al. (2010) SOX9 is a major negative regulator of cartilage vascularization, bone marrow formation and endochondral ossification. *Development* 137: 901–911.
43. Nishimura R, Wakabayashi M, Hata K, Matsubara T, Honma S, et al. (2012) Osterix regulates calcification and degradation of chondrogenic matrices through matrix metalloproteinase 13 (MMP13) expression in association with transcription factor Runx2 during endochondral ossification. *J Biol Chem* 287: 33179–33190.
44. Friedman SL (2003) Liver fibrosis – from bench to bedside. *J Hepatol* 38 Suppl 1: S38–53.
45. Endo H, Niioka M, Sugioka Y, Itoh J, Kameyama K, et al. (2011) Matrix metalloproteinase-13 promotes recovery from experimental liver cirrhosis in rats. *Pathobiology* 78: 239–252.
46. Kim EJ, Cho HJ, Park D, Kim JY, Kim YB, et al. (2011) Antifibrotic effect of MMP13-encoding plasmid DNA delivered using polyethylenimine shielded with hyaluronic acid. *Mol Ther* 19: 355–361.